

**Ion mobility mass spectrometry for ion recovery and clean-up of MS and MS/MS spectra  
obtained from low abundance viral samples**

David J. Harvey<sup>1,2</sup>, Max Crispin<sup>1</sup>, Camille Bonomelli<sup>1</sup>, Jim H. Scrivens<sup>2</sup>.

1) Oxford Glycobiology Institute, Department of Biochemistry, University of Oxford, South Parks Road,  
Oxford, OX1 3QU, UK.

2) Department of Biological Sciences, University of Warwick, Coventry, CV47AL, UK.

**Running title**

Ion mobility MS and CID of viral glycans

**Keywords:** *N*-glycans, ion mobility, CID, contamination.

**Address reprint requests to:**

Dr David J. Harvey,  
Oxford Glycobiology Institute,  
Department of Biochemistry,  
South Parks Road, Oxford,  
OX1 3QU, UK.  
Tel. (44) (0) 1865 275750  
Fax. (44) (0) 1865 275216  
e-mail [david.harvey@bioch.ox.ac.uk](mailto:david.harvey@bioch.ox.ac.uk)

**Abstract**

Many samples of complex mixtures of *N*-glycans released from small amounts of material, such as glycoproteins from viruses, present problems for mass spectrometric analysis because of the presence of contaminating material that is difficult to remove by conventional methods without involving sample loss. This paper describes the use of ion mobility for extraction of glycan profiles from such samples and for obtaining clean CID spectra when targeted *m/z* values capture additional ions from those of the target compound. *N*-Glycans were released enzymatically from within SDS-PAGE gels, from the representative glycoprotein, gp120 of the human immunodeficiency virus, and examined by direct infusion electrospray in negative mode followed by ion mobility with a Waters Synapt G2 mass spectrometer. Clean profiles of singly, doubly and triply charged *N*-glycans were obtained from samples in cases where the raw electrospray spectra displayed only a few glycan ions as the result of low sample concentration or the presence of contamination. Ion mobility also enabled uncontaminated CID spectra to be obtained from glycans when their molecular ions displayed coincidence with ions from fragments or multiply charged ions with similar *m/z* values. This technique proved to be invaluable for removing extraneous ions from many CID spectra. The presence of such ions often produces spectra that are difficult to interpret. Most CID spectra, even those from abundant glycan constituents, benefited from such clean-up showing that the extra dimension provided by ion mobility was invaluable for studies of this type.

## Introduction

Mixtures of *N*-Glycans released from glycoproteins frequently contain contaminants such as polymers, residual buffers and salts that inhibit ionization of the target compounds or produce ions that mask those from the glycans. This situation is frequently encountered with the small amounts of material that are released in-gel from SDS-PAGE-separated glycoproteins from, for example, viral glycoproteins [1-4]. Such contamination is often difficult to remove by traditional wet chemistry methods without sample loss. Pre-mass spectral fractionation such as, for example, the use of HPLC in LC/MS systems can reduce this problem considerably, but contamination issues remain problematic with direct infusion techniques or those using MALDI ionization. Furthermore, electrospray spectra are characterized by the production of multiply charged ions, often in several charge states from a single compound and fragmentation can occur in the ion source or other regions of the instrument, further complicating the spectra. Under these conditions, ions selected for CID frequently include contributions from other ions with equivalent *m/z* values arising from these mechanisms, often leading to ambiguous spectra or, in the worst case, rendering the spectra uninterpretable.

We have been investigating the use of ion mobility to address these problems in situations where chromatographic inlets to the mass spectrometer are not available. Ion mobility can be regarded as an orthogonal technique to chromatography with the advantage that separations can be performed in milliseconds rather than the tens of minutes normally required for chromatography and one which offers the possibility of reducing sample losses because of the reduced need for pre-mass spectrometric clean-up. In parallel to glucose units that can be used to assign retention data to HPLC peaks, collisional cross sections can be used for glycans. These cross sections can be measured directly with drift tube instruments or indirectly with travelling-wave instruments using suitable callibrants [5-8]. Furthermore, with nanospray infusion, the operator can select specific ions for CID studies rather than relying on data-dependent acquisition to select precursor ions for CID studies. Unfortunately, mass spectrometry suffers from the disadvantage of being unable to separate isomers and other isobaric species, a task that can often be performed by chromatography. Nevertheless instruments fitted with ion mobility analysers have the potential to redress this disparity because ion mobility separation relies on the shape of the molecules as well as mass and charge.

We [3, 9-11] and other investigators have already shown that, in the absence of the extra dimension provided by mass spectrometers fitted with chromatographic inlet systems, ion mobility can be used to advantage to extract ions of interest from samples containing small amounts of material and to display a relatively clean glycan profile [9, 10]. Several investigators [12-18] have shown that lipids, nucleotides, peptides and glycans fall on different mobility:*m/z* bands and can, thus, be separated. By use of this method, for example, singly charged  $[M+Na]^+$  *N*-glycan ions have been separated from mixtures containing various additional adducts and fragments [14]. Vakhrushev *et al.* [19] separated singly- and doubly-charged sialylated *N*-glycan-derived fragment ions with overlapping isotope clusters (*m/z* 1199.93 (doubly charged) and 1200.42) in negative ion mode and demonstrated separation of the deprotonated glycan ions from Neu5Ac<sub>2</sub>-Hex<sub>5</sub>-HexNAc<sub>3</sub> (*m/z* 1008.8, doubly charged) and Neu5Ac<sub>3</sub>-dHex-Hex<sub>6</sub>-HexNAc<sub>5</sub> (*m/z* 1007.3, triply charged) [20].

Ion mobility also has the ability to separate isomers, particularly of small carbohydrates [17, 21-29]. Fenn and McLean [30] showed that some isomeric oligosaccharides from milk could be separated and Williams *et al.* [31] separated Man<sub>3</sub>GlcNAc<sub>3</sub> isomers from ovalbumin and assigned structures based on negative ion fragmentation data. Plasencia *et al.* [32] have observed three peaks from the  $[M+Na_2]^{2+}$  ion of the permethylated glycan of composition Hex<sub>5</sub>HexNAc<sub>4</sub> from the same source. These peaks were assigned structures based on molecular modelling simulations but the structures were not confirmed by fragmentation. Yamaguchi *et al.* [33] partially separated the two isomers of the monogalactosylated biantennary glycans from IgG as 2-aminopyridine derivatives with a Waters Synapt G2 travelling wave instrument (nitrogen drift gas) and, again, modelled these compounds to assign structures. Isomers of Man<sub>7</sub>GlcNAc<sub>2</sub> ionized as the  $[M+Na_2]^{2+}$  ion have been partially separated; in this case the isomers were detected by monitoring selected fragment ions [34]. Both *et al.* [35] have investigated the use of fragment ions, generated in the trap region of a Synapt mass spectrometer (before mobility separation) for differentiating between various isomeric disaccharides. Monosaccharide fragments generated in this manner exhibited similar arrival time distributions (ATDs). Also of interest is the energy-resolved technique introduced by Hoffmann *et al.* [36], that also involved trap fragmentation. Four isomeric trisaccharides with slightly different ATDs were investigated and were shown to fragment at different collision energies allowing selective suppression

of their signals to improve resolution. Larger isomeric glycans have also been resolved; thus Rashid *et al.* [37] have separated  $\alpha$ -1,4-linked maltooligosaccharides with a degree of polymerisation of up to 35 from  $\alpha$ -1,6-linked dextran and  $\alpha$ -1,4/1,6-linked pullulan. Conformers of maltohexaose were also separated. 3-Amino-quinoline-labeled partially methyl-esterified  $\alpha$ -(1,4)-linked galacturonic acid oligosaccharides have also given asymmetrical ATDs attributable to isomers [38]. Complex ATDs for several doubly and triply sodium adducted permethylated *N*-glycans released from human tissues have been observed [26], suggesting isomer separation but the species producing each of the glycan constituents were not determined.

The additional separating power of ion mobility has already found application in medicine and pharmaceuticals. Investigators from Clemmer's group, for example, have used it for differentiating various disease states, particularly cancer, by examination of *N*-glycans from serum glycoproteins [26, 39, 40]. Olivova *et al.* [41] have used travelling-wave ion mobility spectrometry (TWIMS) to separate the heavy and light chains of IgG1; These glycoproteins have similar *m/z* values but different charge states. The analysis allowed the glycoforms of the heavy chain containing differently galactosylated biantennary glycans to be resolved. Several drugs, present in relatively low concentration in various pharmaceutical formulations have been analysed directly using the power of ion mobility to extract the ions from the drugs following ionization by desorption electrospray [42] and Eckers *et al.* [43] have used the technique to detect impurities in formulated drug products. Damen *et al.* [44] have similarly examined lot-to-lot heterogeneity in the *N*-glycosylation profile of the therapeutic monoclonal antibody Trastuzumab. Further applications can be found in reference [45].

The object of the present work is to evaluate the potential of ion mobility for the structural identification of *N*-glycans released from glycoproteins when only small amounts are available. Glycans released from the human immunodeficiency virus-derived glycoprotein, gp120, was used as a representative example. Negative ion methods were used because this ionization technique has been shown to provide more structurally-specific fragment ions than the parallel positive ion techniques [46-50].

## Materials and Methods

### Materials

Recombinant HIV-1 gp120<sub>BG505</sub>, bearing a C-terminal poly-His tag, was expressed transiently from human embryonic kidney 293T cells as described previously [51, 52] and purified by immobilised metal affinity chromatography using a HisTrap HP column (GEHealthcare, Amersham, UK), and concentrated. *N*-linked glycans were released in-gel using the method originally described by Küster *et al.* [53] with the enzyme protein *N*-glycosidase F (PNGase F, EC 3.5.1.52) following separation by SDS-PAGE, extraction by sonication in water and purification with a porous graphitised carbon column (Thermo Scientific, Runcorn, UK). Methanol was obtained from BDH Ltd. (Poole, UK) and ammonium phosphate was from Aldrich Chemical Co. Ltd. (Poole, UK). Dextran from *Leuconostoc mesenteroides* was obtained from Fluka (Poole, UK).

### Sample Preparation for mass spectrometry

Following release from the glycoproteins, the glycans (1  $\mu$ l samples of aqueous solution) were cleaned with a Nafion 117 membrane as described by Börnsen *et al.* [54]. They were diluted with water (4  $\mu$ l), and methanol (6  $\mu$ l) plus 1  $\mu$ l of an aqueous solution of ammonium phosphate (0.05 M, to maximize formation of  $[M+H_2PO_4]^-$  ions, (the ions usually encountered from biological samples)). Samples were then centrifuged at 10,000 rpm (9503 x g) for 1 min to sediment any particulates.

### Electrospray, Ion Mobility Mass Spectrometry

Travelling wave ion mobility experiments were carried out with a Waters Synapt G2 travelling wave ion mobility mass spectrometer (TWIMS) (Waters MS-Technologies, Manchester, UK) fitted with an electrospray (ESI) ion source. Samples were infused through Waters thin-wall nanospray capillaries. Ion source conditions were: ESI capillary voltage, 1.2 kV cone voltage, 100 V, ion source temperature 80°C. The T-wave velocity and peak height voltages were 450 m/sec and 40 V respectively. The T-wave mobility cell contained nitrogen and was operated at a pressure of 0.55 mbar. Fragmentation was performed after mobility separation in the transfer cell with argon as the collision gas. The instrument was externally mass calibrated with sialylated *N*-glycans released from bovine fetuin [55] and the ion mobility cell was calibrated with dextran from *Leuconostoc mesenteroides*. Data acquisition and processing were carried out using the Waters Driftscope (version 2.1) software and MassLynx<sup>TM</sup> (version 4.0). CID spectra were interpreted according to previously published data [46-50] and further confirmation of structure was made by comparing collision cross sections with those of

reference glycans [7]. The scheme devised by Domon and Costello [56] was used to name the fragment ions.

## Results and Discussion

### MS Spectra

As an example of the use of ion mobility to extract glycan ions from spectra derived from low abundance samples following an in-gel release with PNGase F [53], *N*-Glycans were released in-gel from the glycoprotein gp120 and two typical ESI spectra are shown in Figure 1b and c. The spectrum in panel b is of a reasonably concentrated sample but that in panel c is of a sample with low concentrations of glycans (released in gel from about 5  $\mu$ g of glycoprotein) and with a high background which obscures most of the glycan ions. However, the glycan ions from this latter sample could be separated by ion mobility as shown in the  $m/z$ /drift time plot in Figure 1a (DriftScope display). The circled region labelled 1 contains the singly charged ions, mainly as phosphate adducts. These ions were selected and exported to MassLynx to give the spectrum shown in Figure 1d. Most of the noise has been removed allowing some minor constituents to be seen. Some of these glycans have been characterized in earlier publications [9-11, 53] and the structures of all but the minor constituents were confirmed by negative ion CID using fragmentation in the transfer cell of the Synapt instrument (after mobility separation) [46-50] and cross section measurements [7]. The main diagnostic ions in the negative ion CID spectra can be summarized as follows. Location of the core fucose was reflected in the  $^{2,4}A$  ion from the reducing-terminal GlcNAc residue (see Figure 2 for an example); the two triantennary glycans were identified by the presence of a fragment at  $m/z$  831 (3-branched isomer) and  $m/z$  1053 (D ion (formed by loss of the chitobiose core and 3-antenna)), 1035 and 1017 (6-branched isomer) [57]; bisected glycans gave a prominent fragment formed by loss of GlcNAc from the D-ion. Sialic acid linkages were identified by the method reported by Wheeler *et al.* [58]. Identified glycans are listed in Table 1 with their structures in Scheme 1. Many of the glycans were detected in different ionic states, i.e. various combinations of deprotonated molecules, sodium salts and phosphate adducts.

The spectrum in Figure 1e is of the doubly charged ions extracted from region 2 of the DriftScope display (Figure 1a) from the low abundance sample and Figure 1f is that of the triply charged ions. The glycans in the doubly and triply charged spectra were the larger high-mannose compounds as diphosphate adducts and di-, tri- and tetra-sialylated di-, tri- and tetra-antennary complex glycans as deprotonated ions. Ions at the  $m/z$  1250.8 and 1347.8, not seen in earlier studies, corresponded to tri- and tetra-sialylated glycans with poly-*N*-acetylactosamine extensions to their antennae (Compounds **73** and **74**, Scheme 1). This analysis, therefore, allowed glycan ions that were obscured by the contamination to be visualized and, consequently, they could be fragmented in the transfer cell. However, because of the presence of the contaminating ions, in some cases, species other than the targeted glycan ions were also selected leading to extraneous ions in the CID spectra making them difficult to interpret, particularly when the target ions were present in low abundance. Ion mobility was then used again to remove these contaminating ions as described below.

### CID spectra

#### **Structural information from glycans of low abundance whose masses coincide with those of other compounds**

It is clear from Figure 1a that selection for CID of the molecular ions from most of the singly charged glycans would also include several other ions from the background and from regions 2 and 3. Such a spectrum is shown in Figure 2a. The target glycan is of a mixture of the monogalactosylated biantennary glycans **29** and **30** (Scheme 1) of  $m/z$  1721 (phosphate adducts) from the low abundance sample. The mass of the parent ions are the same as that of the first isotope peak from the  $^{2,4}A_6$  fragment ion of the high-mannose glycan  $\text{Man}_9\text{GlcNAc}_2$  (**44**) and ions from both sources are present in the spectrum. After ion mobility separation, the arrival time distribution (ATD) profile of this ion is asymmetric (Inset to Figure 2a) and when spectra were extracted from each side of this peak, as shown by the horizontal lines in the inset, relatively clean spectra of the target glycans,  $\text{Gal}_1\text{Man}_3\text{GlcNAc}_4\text{Fuc}_1$  (Figure 2b) and of the fragment ion (Figure 2c) were obtained. In spectrum 2b, the ions at  $m/z$  424 ( $\text{Gal-GlcNAc-CH=CH}_2\text{-O}^-$ ) and 262 ( $\text{GlcNAc-CH=CH}_2\text{-O}^-$ ) define the compositions of the two antennae and the distribution of the galactose residue between the antennae is defined by the D (loss of the 3-antenna and chitobiose core) and D-18 ions at  $m/z$  526/508 (no galactose on the 6-antenna) and  $m/z$  688/670 (galactose on the 6-antenna). Corresponding spectra from the other, more abundant sample (Figure 1b) where the  $\text{Gal}_1\text{Man}_3\text{GlcNAc}_4\text{Fuc}_1$  glycan (**29**, **30**) was relatively more abundant is shown in Figures 2d and 2e so that these features can be seen more clearly.

However, it can be seen that even when the concentration of glycans such as **29** and **30** are very low and coincident with ions from other sources, it can still be possible to extract structural information using ion mobility and negative ion fragmentation.

Even with the more abundant glycans, the CID spectra still benefitted from ion mobility clean-up, as shown in Figure 3 where ion mobility has effectively removed contamination ions in the low mass region. Panel a shows the total ESI spectrum of the high-mannose glycan  $\text{Man}_9\text{GlcNAc}_2$  (**44**) and panel b shows the mobility-extracted fragment ions from the region of the large peak in the inset to panel c (100-150 msec region). The lower panel of this inset shows the DriftScope image with the ATD profile (labelled b) in the upper panel. The main spectrum in panel c of Figure 3 is of the extracted contaminating ions (region from 0-80 msec of the DriftScope display).

#### ***Use of ion mobility to separate isobaric compounds***

Figure 4 shows the CID spectrum of the glycan(s) of mass 1534.5 from the high abundance sample having the composition  $\text{Hex}_5\text{GlcNAc}_3$ . Fragment ions are inconsistent with the presence of a single compound: those at  $m/z$  647 (D), 629 (D-18), 575 ( $^{0.3}\text{A}_3$ ) and 545 ( $^{2.4}\text{A}_3$ ) indicate the presence of a compound with three mannose residues in the 6-antenna (compound **50**), whereas the ion at  $m/z$  424 which contains a Gal-GlcNAc moiety, leaves only two remaining mannose residues for the 6-antenna (compound **11**), assuming that the molecules both contained the common trimannosyl-chitobiose core. That these two compounds are present is consistent with the bimodal ATD peak (Inset to Figure 4a, red trace) and their presence was confirmed by extracting the spectra from each side of the peak to give the spectra shown in Figures 4b and 4c. ATD plots of the mass-different diagnostic fragment ions [25, 27, 34, 59-62] for these two compounds (blue and green traces for selected ions from compounds **11** and **10** respectively) maximized separately under the two peaks of the total ATD profile, further confirming the presence of these two compounds. This technique can also be used to identify the presence of isomeric high-mannose isomers and will be the subject of a future communication.

#### ***Use of ion mobility to extract spectra of multiple glycans when CID selects ions of different composition but with the same $m/z$ value***

A common problem with acquisition of CID spectra from constituents in mixtures, particularly when they are present at low abundance, is the presence of several species exhibiting the same  $m/z$  value all of which contribute fragment ions to the CID spectrum. Even the spectra of relatively abundant species can also be affected by this problem. For example, the CID spectrum of the ion at  $m/z$  1007 (Figure 5a) from the high abundance HIV sample, targeted for the phosphate adduct (singly charged) of the glycan  $\text{Man}_3\text{GlcNAc}_2$  (**1**), contains many additional ions, particularly above the mass of the parent ion, making the spectrum difficult to interpret. The Driftscope analysis (Figure 6) shows the presence of at least three compounds that fragment in the transfer region of the instrument (regions labelled 1-3 in Figure 6) and several compounds that have fragmented prior to mobility separation (regions 4, 5 and 6). The spectra of these regions are shown in Figure 5b-g respectively. A clean spectrum of the target compound,  $\text{Man}_3\text{GlcNAc}_2$  (**1**) was extracted from region 1 and is shown in Spectrum 5b. Spectrum 5d from region 3 is from the triply charged ion from the glycan of composition  $\text{Hex}_6\text{HexNAc}_5\text{dHex}_1\text{Neu5Ac}_3$  (**61**, **62**). The major fragment ion at  $m/z$  290 in this spectrum is the  $\text{B}_1$  ion consisting of sialic acid and the singly charged ion at  $m/z$  2441.8 is formed by loss of two sialic acids. The ion at  $m/z$  2340.8 is the corresponding  $^{0.2}\text{A}_7$  ion, typical for compounds of this type. The rather poor spectrum is probably the result of the collision energy (transfer voltage 66.7 V) being set to be appropriate for the targeted singly charged ion of  $\text{Man}_3\text{GlcNAc}_2$  (Spectrum 5b) and which is too high from optimal fragmentation of the triply charged species and has caused extensive loss of two sialic acids. A voltage of 55 V would be more appropriate for the full spectrum to be recovered as demonstrated by a spectrum from a parallel sample (Inset to Figure 5d) recorded with this voltage. The virtual absence of the doubly charged ions at  $m/z$  1366 and 1315 representing loss of one sialic acid and formation of the corresponding  $^{0.2}\text{A}_7$  ion after ion selection and before mobility separation, produces the spectrum in region 5 (Spectrum 5f). The spectrum in region 6 (Figure 5g) is that from the loss of two sialic acids ( $m/z$  2241). Losses of sialic acid by fragmentation within the instrument and, presumably also in the ion source region, questions the quantitative relationship between the various sialylated species shown in the MS spectra (Figure 1d and e) and suggests that stabilization of the sialic acids by methylation [63, 64] or amidation [65] or analysis by HPLC should be employed to obtain this information.

The spectrum in Figure 5c (region 2) is of a doubly charged ion. The fragments are singly charged with prominent peaks at  $m/z$  1558, 1498 and 1355 corresponding to the  $^{2,4}A_6$ ,  $B_5$  and  $^{2,4}A_5$  ions from  $\text{Man}_8\text{GlcNAc}_2$  (**34**). A tri-phosphate adduct (doubly charged) from this compound would have a mass of  $m/z$  1006.25 which would fall within the 4  $m/z$  mass window used to select  $m/z$  1007 for fragmentation. The unstable nature of this species is possibly reflected by the prominent ion at  $m/z$  1817 (singly charged) in spectrum 5e from region 4 which corresponds to the monophosphate adduct of this high-mannose glycan.

## Conclusion

From the above results, it can be seen that ion mobility can be used in a number of ways to aid structural determination of *N*-glycans, particularly when they occur at low concentration or in contaminated samples. Extraction of ions in different charge states can often eliminate contamination such as polyethylene glycol [10] and can reveal the presence of minor compounds whose molecular ions are masked by ions from major compounds in different charge states but with different  $m/z$  values.

CID spectra can also be improved. Simply selecting an ion for CID analysis from complex mixtures can lead to contaminated spectra. Much of this contamination can be removed by the additional stage of ion mobility. Clearly, there are other methods, such as HPLC, of cleaning samples prior to CID but, in the absence of such techniques, for example when MALDI is used as the ionization technique, ion mobility provides a simple method for achieving similar results. Less contamination would be introduced into the MS/MS spectra if the ion selection window was reduced to a width of only 1 Da. However, we have frequently found with samples such as the ones analysed here, it is advantageous to use a wider window so that isotopic peaks are displayed in order to aid identification of other adducts of the glycans, such as the chloride adduct. Although we routinely add phosphate to the sample in an attempt to form only the phosphate adducts, the final spectrum will depend to a large extent on the original composition of the sample. Furthermore, using a narrower mass selection window often compromises sensitivity and maximum sensitivity is normally required in the analysis of glycans derived from gel-separated glycoproteins. Our philosophy is to use the minimum of pre-MS clean-up in order to minimize sample losses and to use the mass spectrometer at its full potential. The extra dimension provided by ion mobility is invaluable in this context.

Thirdly, the presence of isobaric and isomeric compounds can be revealed by plotting the ATD profiles of diagnostic fragment ions. These plots frequently reveal slightly different drift times from the constituents in cases where the overall ATD profile only suggests their presence by slight asymmetry or broadening. Negative ion spectra are particularly appropriate because they usually contain diagnostic ions that differ in mass between the isobaric compounds.

Finally, although not discussed here, ion mobility data can be described by cross section values that provide an additional physical property that can assist compound identification and which can be incorporated into databases for more automated analyses of complex glycan profiles. Clearly, therefore, ion mobility provides extra dimensions of analysis and should considerably help in the future analyses of *N*-glycans, particularly when sample amounts are limiting.

## Acknowledgements

We thank Professor Raymond Dwek, FRS, for his continued help and support and the Oxford Glycobiology Bequest for funding. This study was supported by grants from CHAVI-ID, IAVI and NAC CAVD.

## References

- 1 Bonomelli, C., Doores, K. J., Dunlop, D. C., Thaney, V., Dwek, R. A., Burton, D. R., Crispin, M., Scanlan, C. N.: The glycan shield of HIV is predominantly oligomannose independently of production system or viral clade. *PLoS One* 6, e23521 (2011).
- 2 Crispin, M., Harvey, D. J., Bitto, D., Bonomelli, C., Edgeworth, M., Scrivens, J. H., Huiskonen, J. T., Bowden, T. A.: Structural plasticity of the Semliki Forest virus glycome upon interspecies transmission. *J. Proteome Res.* 13, 1702–1712 (2014).
- 3 Crispin, M., Harvey, D. J., Bitto, D., Halldorsson, S., Bonomelli, C., Edgeworth, M., Scrivens, J. H., Huiskonen, J. T., Bowden, T. A.: Uukuniemi phlebovirus assembly and secretion leave a functional imprint on the virion glycome. *J. Virol.* 88, 10244–10251 (2014).
- 4 Doores, K. J., Bonomelli, C., Harvey, D. J., Vasiljevic, S., Dwek, R. A., Burton, D. R., Crispin, M., Scanlan, C. N.: Envelope glycans of immunodeficiency virions are almost entirely oligomannose antigens. *Proc. Natl. Acad. Sci., USA* 107, 13800–13805 (2010).
- 5 Bush, M. F., Hall, Z., Giles, K., Hoyes, J., Robinson, C. V., Ruotolo, B. T.: Collision cross sections of proteins and their complexes: A calibration framework and database for gas-phase structural biology. *Anal. Chem.* 82, 9557–9565 (2010).
- 6 Sivalingam, G. N., Yan, J., Sahota, H., Thalassinios, K.: Amphitrite: a program for processing travelling wave ion mobility mass spectrometry data. *Int. J. Mass Spectrom.* 345–347, 54–62 (2013).
- 7 Hofmann, J., Struwe, W. B., Scarff, C. A., Scrivens, J. H., Harvey, D. J., Pagel, K.: Estimating collision cross sections of negatively charged *N*-glycans using travelling wave ion mobility-mass spectrometry. *Anal. Chem.* 86, 10789–10795 (2014).
- 8 Pagel, K., Harvey, D. J.: Ion mobility mass spectrometry of complex carbohydrates - collision cross sections of sodiated *N*-linked glycans. *Anal. Chem.* 85, 5138–5145 (2013).
- 9 Harvey, D. J., Sobott, F., Crispin, M., Wrobel, A., Bonomelli, C., Vasiljevic, S., Scanlan, C. N., Scarff, C., Thalassinios, K., Scrivens, J. H.: Ion mobility mass spectrometry for extracting spectra of *N*-glycans directly from incubation mixtures following glycan release: Application to glycans from engineered glycoforms of intact, folded HIV gp120. *J. Am. Soc. Mass Spectrom.* 22, 568–581 (2011).
- 10 Harvey, D. J., Scarff, C. A., Edgeworth, M., Crispin, M., Scanlan, C. N., Sobott, F., Allman, S., Baruah, K., Pritchard, L., Scrivens, J. H.: Travelling wave ion mobility and negative ion fragmentation for the structural determination of *N*-linked glycans. *Electrophoresis* 34, 2368–2378 (2013).
- 11 Harvey, D. J., Scarff, C. A., Crispin, M., Scanlan, C. N., Bonomelli, C., Scrivens, J. H.: MALDI-MS/MS with traveling wave ion mobility for the structural analysis of *N*-linked glycans. *J. Am. Soc. Mass Spectrom.* 23, 1955–1966 (2012).
- 12 Fenn, L. S., McLean, J. A.: Biomolecular structural separations by ion mobility–mass spectrometry. *Anal. Bioanal. Chem.* 391, 905–909 (2008).
- 13 Fenn, L. S., Kliman, M., Mahsut, A., Zhao, S. R., McLean, J. A.: Characterizing ion mobility-mass spectrometry conformation space for the analysis of complex biological samples. *Anal. Bioanal. Chem.* 394, 235–244 (2009).
- 14 Fenn, L. S., McLean, J. A.: Simultaneous glycoproteomics on the basis of structure using ion mobility-mass spectrometry. *Mol. Biosyst.* 5, 1298–1232 (2009).
- 15 Woods, A. S., Ugarov, M., Egan, T., Koomen, J., Gillig, K. J., Fuhrer, K., Gonin, M., Schultz, J. A.: Lipid/peptide/nucleotide separation with MALDI-ion mobility-TOF MS. *Anal. Chem.* 76, 2187–2195 (2004).
- 16 Kaplan, K., Jackson, S., Dwivedi, P., Davidson, W. S., Yang, Q., Tso, P., Siems, W., Woods, A., Hill Jr., H. H.: Monitoring dynamic changes in lymph metabolome of fasting and fed rats by matrix-assisted laser desorption/ionization-ion mobility mass spectrometry (MALDI-IMMS). *Int. J. Ion Mobil. Spectrom.* 16, 177–184 (2013).
- 17 Li, H., Bendiak, B., Siems, W. F., Gang, D. R., Hill, J., Herbert H.: Carbohydrate structure characterization by tandem ion mobility mass spectrometry (IMMS)<sup>2</sup>. *Anal. Chem.* 85, 2760–2769 (2013).
- 18 May, J. C., Goodwin, C. R., Lareau, N. M., Leaptrot, K. L., Morris, C. B., Kurulugama, R. T., Mordehai, A., Klein, C., Barry, W., Darland, E., Overney, G., Imatani, K., Stafford, G. C., Fjeldsted, J. C., McLean, J. A.: Conformational ordering of biomolecules in the gas phase: Nitrogen collision cross sections measured on a prototype high resolution drift tube ion mobility-mass spectrometer. *Anal. Chem.* 86, 2107–2116 (2014).



- 19 Vakhrushev, S. Y., Langridge, J., Campuzano, I., Hughes, C., Peter-Katalinić, J.: Identification of monosialylated *N*-glycoforms in the CDG urinome by ion mobility tandem mass spectrometry: The potential for clinical applications. *Clin. Proteomics* 4, 47-57 (2008).
- 20 Vakhrushev, S. Y., Langridge, J., Campuzano, I., Hughes, C., Peter-Katalinic, J.: Ion mobility mass spectrometry analysis of human glycourinome. *Anal. Chem.* 80, 2506-2513 (2008).
- 21 Clowers, B. H., Dwivedi, P., Steiner, W. E., Hill, H. H. J., Bendiak, B.: Separation of sodiated isobaric disaccharides and trisaccharides using electrospray ionization-atmospheric pressure ion mobility-time of flight mass spectrometry. *J. Am. Soc. Mass Spectrom.* 16, 660-669 (2005).
- 22 Dwivedi, P., Bendiak, B., Clowers, B. H., Hill, H. H. J.: Rapid resolution of carbohydrate isomers by electrospray ionization ambient pressure ion mobility spectrometry-time-of-flight mass spectrometry (ESI-APIMS-TOFMS). *J. Am. Soc. Mass Spectrom.* 18, 1163-1175 (2007).
- 23 Huang, Y., Dodds, E. D.: Ion mobility studies of carbohydrates as group I adducts: Isomer specific collisional cross section dependence on metal ion radius. *Anal. Chem.* 85, 9728-9735 (2013).
- 24 Li, H., Giles, K., Bendiak, B., Kaplan, K., Siems, W. F., Hill, H. H., Jr.: Resolving structural isomers of monosaccharide methyl glycosides using drift tube and traveling wave ion mobility mass spectrometry. *Anal. Chem.* 84, 3231-3239 (2012).
- 25 Li, H., Bendiak, B., Siems, W. F., Gang, D. R., Hill, J., Herbert H.: Ion mobility mass spectrometry analysis of isomeric disaccharide precursor, product and cluster ions. *Rapid Commun. Mass Spectrom.* 27, 2699-2709 (2013).
- 26 Gaye, M. M., Valentine, S. J., Hu, Y., Mirjankar, N., Hammoud, Z. T., Mechref, Y., Lavine, B. K., Clemmer, D. E.: Ion mobility-mass spectrometry analysis of serum *N*-linked glycans from esophageal adenocarcinoma phenotypes. *J. Proteome Res.* 11, 6102-6110 (2012).
- 27 Lee, S., Valentine, S. J., Reilly, J. P., Clemmer, D. E.: Analyzing a mixture of disaccharides by IMS-VUVPD-MS. *Int. J. Mass Spectrom.* 309, 161- 167 (2012).
- 28 Yamagaki, T., Sato, A.: Isomeric oligosaccharides analyses using negative-ion electrospray ionization ion mobility spectrometry combined with collision-induced dissociation MS/MS. *Anal. Sci.* 25, 985-988 (2009).
- 29 Zhu, M., Bendiak, B., Clowers, B., Hill, H. H.: Ion mobility-mass spectrometry analysis of isomeric carbohydrate precursor ions. *Anal. Bioanal. Chem.* 394, 1853-1867 (2009).
- 30 Fenn, L. S., McLean, J. A.: Structural resolution of carbohydrate positional and structural isomers based on gas-phase ion mobility-mass spectrometry. *Phys. Chem. Chem. Phys.* 13, 2196-2205 (2011).
- 31 Williams, J. P., Grabenauer, M., Carpenter, C. J., Holland, R. J., Wormald, M. R., Giles, K., Harvey, D. J., Bateman, R. H., Scrivens, J. H., Bowers, M. T.: Characterization of simple isomeric oligosaccharides and the rapid separation of glycan mixtures by ion mobility mass spectrometry. *Int. J. Mass Spectrom.* 298, 119-127 (2010).
- 32 Plasencia, M. D., Isailovic, D., Merenbloom, S. I., Mechref, Y., Clemmer, D. E.: Resolving and assigning *N*-linked glycan structural isomers from ovalbumin by IMS-MS. *J. Am. Soc. Mass Spectrom.* 19, 1706-1715 (2008).
- 33 Yamaguchi, Y., Nishima, W., Re, S., Sugita, Y.: Confident identification of isomeric *N*-glycan structures by combined ion mobility mass spectrometry and hydrophilic interaction liquid chromatography. *Rapid Commun. Mass Spectrom.* 26, 2877-2884 (2012).
- 34 Zhu, F., Lee, S., Valentine, S. J., Reilly, J. P., Clemmer, D. E.: Mannose7 glycan isomer characterization by IMS-MS/MS analysis. *J. Am. Soc. Mass Spectrom.* 23, 2158-2166 (2012).
- 35 Both, P., Green, A. P., Gray, C. J., Šardžik, R., Voglmeir, J., Fontana, C., Austeri, M., Rejzek, M., Richardson, D., Field, R. A., Widmalm, G., Flitsch, S. L., Evers, C. E.: Discrimination of epimeric glycans and glycopeptides using IM-MS and its potential for carbohydrate sequencing. *Nat. Chem.* 6, 65-74 (2014).
- 36 Hoffmann, W., Hofmann, J., Pagel, K.: Energy-resolved ion mobility-mass spectrometry - A concept to improve the separation of isomeric carbohydrates. *J. Am. Soc. Mass Spectrom.* 25, 471-479 (2014).
- 37 Rashid, A. M., Saalbach, G., Bornemann, S.: Discrimination of large maltooligosaccharides from isobaric dextran and pullulan using ion mobility mass spectrometry. *Rapid Commun. Mass Spectrom.* 28, 191-199 (2014).
- 38 Leijdekkers, A. G. M., Huang, J.-H., Bakx, E. J., Gruppen, H., Schols, H. A.: Identification of novel isomeric pectic oligosaccharides using hydrophilic interaction chromatography coupled to traveling-wave ion mobility mass spectrometry. *Carbohydr. Res.*, In Press (2015).

- 39 Isailovic, D., Kurulugama, R. T., Plasencia, M. D., Stokes, S. T., Kyselova, Z., Goldman, R., Mechref, Y., Novotny, M. V., Clemmer, D. E.: Profiling of human serum glycans associated with liver cancer and cirrhosis by IMS-MS. *J. Proteome Res.* 7, 1109-1117 (2008).
- 40 Isailovic, D., Plasencia, M. D., Gaye, M. M., Stokes, S. T., Kurulugama, R. T., Pungpapong, V., Zhang, M., Kyselova, Z., Goldman, R., Mechref, Y., Novotny, M. V., Clemmer, D. E.: Delineating diseases by IMS-MS profiling of serum *N*-linked glycans. *J. Proteome Res.* 11, 576-585 (2012).
- 41 Olivova, P., Chen, W., Chakraborty, A. B., Gebler, J. C.: Determination of *N*-glycosylation sites and site heterogeneity in a monoclonal antibody by electrospray quadrupole ion-mobility time-of-flight mass spectrometry. *Rapid Commun. Mass Spectrom.* 22, 29-40 (2008).
- 42 Weston, D. J., Bateman, R., Wilson, I. D., Wood, T. R., Creaser, C. S.: Direct analysis of pharmaceutical drug formulations using ion mobility spectrometry/quadrupole-time-of-flight mass spectrometry combined with desorption electrospray ionization. *Anal. Chem.* 77, 7572-7580 (2005).
- 43 Eckers, C., Laures, A. M.-F., Giles, K., Major, H., Pringle, S.: Evaluating the utility of ion mobility separation in combination with high-pressure liquid chromatography/mass spectrometry to facilitate detection of trace impurities in formulated drug products. *Rapid Commun. Mass Spectrom.* 21, 1255-1263 (2007).
- 44 Damen, C. W. N., Chen, W., Chakraborty, A. B., van Oosterhout, M., Mazzeo, J. R., Gebler, J. C., Schellens, J. H. M., Rosing, H., Beijnen, J. H.: Electrospray ionization quadrupole ion-mobility time-of-flight mass spectrometry as a tool to distinguish the lot-to-lot heterogeneity in *N*-glycosylation profile of the therapeutic monoclonal antibody Trastuzumab. *J. Am. Soc. Mass Spectrom.* 20, 2021-2033 (2009).
- 45 Huang, Y., Gelb, S. A., Dodds, E. D.: Carbohydrate and glycoconjugate analysis by ion mobility mass spectrometry: Opportunities and challenges. *Current Metabolomics* 1, 291-305 (2013).
- 46 Harvey, D. J.: Fragmentation of negative ions from carbohydrates: Part 2, Fragmentation of high-mannose *N*-linked glycans. *J. Am. Soc. Mass Spectrom.* 16, 631-646 (2005).
- 47 Harvey, D. J.: Fragmentation of negative ions from carbohydrates: Part 1; Use of nitrate and other anionic adducts for the production of negative ion electrospray spectra from *N*-linked carbohydrates. *J. Am. Soc. Mass Spectrom.* 16, 622-630 (2005).
- 48 Harvey, D. J.: Fragmentation of negative ions from carbohydrates: Part 3, Fragmentation of hybrid and complex *N*-linked glycans. *J. Am. Soc. Mass Spectrom.* 16, 647-659 (2005).
- 49 Harvey, D. J., Royle, L., Radcliffe, C. M., Rudd, P. M., Dwek, R. A.: Structural and quantitative analysis of *N*-linked glycans by MALDI and negative ion nanospray mass spectrometry. *Anal. Biochem.* 376, 44-60 (2008).
- 50 Harvey, D. J., Rudd, P. M.: Fragmentation of negative ions from *N*-linked carbohydrates. Part 5: Anionic *N*-linked glycans. *Int. J. Mass Spectrom.* 305, 120-130 (2011).
- 51 Aricescu, A. R., Lu, W., Jones, E. Y.: A time- and cost-efficient system for high-level protein production in mammalian cells. *Acta Crystallogr. D Biol. Crystallogr.* 62, 1243-1250 (2006).
- 52 Dunlop, D. C., Bonomelli, C., Mansab, F., Vasiljevic, S., Doores, K. J., Wormald, M. R., Palma, A. S., Feizi, T., Harvey, D. J., Dwek, R. A., Crispin, M., Scanlan, C. N.: Polysaccharide mimicry of the epitope of the broadly neutralizing anti-HIV antibody, 2G12, induces enhanced antibody responses to self oligomannose glycans. *Glycobiology* 20, 812-823 (2010).
- 53 Küster, B., Wheeler, S. F., Hunter, A. P., Dwek, R. A., Harvey, D. J.: Sequencing of *N*-linked oligosaccharides directly from protein gels: In-gel deglycosylation followed by matrix-assisted laser desorption/ionization mass spectrometry and normal-phase high performance liquid chromatography. *Anal. Biochem.* 250, 82-101 (1997).
- 54 Börnsen, K. O., Mohr, M. D., Widmer, H. M.: Ion exchange and purification of carbohydrates on a Nafion<sup>®</sup> membrane as a new sample pretreatment for matrix-assisted laser desorption-ionization mass spectrometry. *Rapid Commun. Mass Spectrom.* 9, 1031-1034 (1995).
- 55 Green, E. D., Adelt, G., Baenziger, J. U., Wilson, S., van Halbeek, H.: The asparagine-linked oligosaccharides on bovine fetuin. Structural analysis of *N*-glycanase-released oligosaccharides by 500- Megahertz <sup>1</sup>H-NMR spectroscopy. *J. Biol. Chem.* 263, 18253-18268 (1988).
- 56 Domon, B., Costello, C. E.: A systematic nomenclature for carbohydrate fragmentations in FAB-MS/MS spectra of glycoconjugates. *Glycoconj. J.* 5, 397-409 (1988).
- 57 Harvey, D. J., Crispin, M., Scanlan, C., Singer, B. B., Lucka, L., Chang, V. T., Radcliffe, C. M., Thobhani, S., Yuen, C.-T., Rudd, P. M.: Differentiation between isomeric triantennary *N*-linked

- glycans by negative ion tandem mass spectrometry and confirmation of glycans containing galactose attached to the bisecting ( $\beta$ 1-4-GlcNAc) residue in *N*-glycans from IgG. *Rapid Commun. Mass Spectrom.* 22, 1047-1052 (2008).
- 58 Wheeler, S. F., Harvey, D. J.: Negative ion mass spectrometry of sialylated carbohydrates: Discrimination of *N*-acetylneuraminic acid linkages by matrix-assisted laser desorption/ionization-time-of-flight and electrospray-time-of-flight mass spectrometry. *Anal. Chem.* 72, 5027-5039 (2000).
- 59 Harvey, D. J., Scrivens, J., Holland, R., Williams, J. P., Wormald, M. R.: Ion-mobility separation coupled with negative ion fragmentation of *N*-linked carbohydrates. *Proceedings of the 56<sup>th</sup> ASMS Conference on Mass Spectrometry*, Denver, CO, USA, Proceedings CD, MOG 09.10 am (2008).
- 60 Lee, S., Li, Z., Valentine, S. J., Zucker, S. M., Webber, N., Reilly, J. P., Clemmer, D. E.: Extracted fragment ion mobility distributions: A new method for complex mixture analysis. *Int. J. Mass Spectrom.* 309, 154- 160 (2012).
- 61 Winkler, W., Huber, W., Vlasak, R., Allmaier, G.: Positive and negative electrospray ionisation travelling wave ion mobility mass spectrometry and low-energy collision-induced dissociation of sialic acid derivatives. *Rapid Commun. Mass Spectrom.* 25, 3235-3244 (2011).
- 62 Brantley, M., Zekavat, B., Harper, B., Mason, R., Solouki, T.: Automated deconvolution of overlapped ion mobility profiles. *J. Am. Soc. Mass Spectrom.* 25, 1810-1819 (2014).
- 63 Powell, A. K., Harvey, D. J.: Stabilisation of sialic acids in *N*-linked oligosaccharides and gangliosides for analysis by positive ion matrix-assisted laser desorption-ionization mass spectrometry. *Rapid Commun. Mass Spectrom.* 10, 1027-1032 (1996).
- 64 Wheeler, S. F., Domann, P., Harvey, D. J.: Derivatization of sialic acids for stabilization in matrix-assisted laser desorption/ionization mass spectrometry and concomitant differentiation of  $\alpha$ (2-3) and  $\alpha$ (2-6) isomers. *Rapid Commun. Mass Spectrom.* 23, 303-312 (2009).
- 65 Zhang, Q., Feng, X., Li, H., Liu, B.-F., Lin, Y., Liu, X.: Methylamidation for isomeric profiling of sialylated glycans by nanoLC-MS. *Anal. Chem.* 86, 7913-7919 (2014).
- 66 Harvey, D. J., Merry, A. H., Royle, L., Campbell, M. P., Dwek, R. A., Rudd, P. M.: Proposal for a standard system for drawing structural diagrams of *N*- and *O*-linked carbohydrates and related compounds. *Proteomics* 9, 3796-3801 (2009).

**Table 1, Masses, compositions, occurrence and structures of the measured ions from gp120.**

Mass <sup>1</sup>	$m/z^2$	Charge	Ion <sup>3</sup>	Sample		Composition				Structure <sup>4</sup>
				1	2	Hex	HexNAc	Fuc	Neu5Ac	
910.3	1007.3	1	a	+	+	3	2	0	0	1
1072.4	1169.4	1	a	+	+	4	2	0	0	2
1234.4	1331.4	1	a	+	+	5	2	0	0	3
1239.5	1356.4	1	a	+	+	3	3	1	0	4
1275.5	1372.5	1	a	+	+	4	3	0	0	5
1316.5	1413.5	1	a	+	-	3	4	0	0	6
1396.5	1493.5	1	a	+	+	6	2	0	0	7
1421.5	1518.5	1	a	+	-	4	3	1	0	8, 9
1437.5	1534.5	1	a	+	+	5	3	0	0	10, 11
	1727.6	1	b	+	+				1	12
1462.5	1559.5	1	a	+	+	3	4	1	0	13
1478.5	1575.5	1	a	+	+	4	4	0	0	14, 15
	1768.6	1	b	+	+				1	16, 17
1519.6	1616.5	1	a	+	-	3	5	0	0	18
	929.8	1	c	+	-					
1558.5	1655.5	1	a	+	+	7	2	0	0	19, 20
	876.2	2	c	+	+					
1583.6	1680.6	1	a	+	+	5	3	1	0	21, 22
	1873.7	1	b	+	+				1	23
1599.6	1696.5	1	a	+	+	6	3	0	0	24
	1889.7	1	b	+	+				1	25
1640.6	1737.6	1	a	+	+	5	4	0	0	26
	1930.8	1	b	+	+				1	27
	1110.4	2	f	+	+				2	28
1624.6	1721.6	1	a	+	+	4	4	1	0	29, 30
	1914.7	1	b	+	+				1	31, 32
1665.6	1762.6	1	a	+	+	3	5	1	0	33
1720.6	1817.6	1	a	+	+	8	2	0	0	34
	957.3	2	c	+	+					
1745.6	1842.6	1	a	+	+	6	3	1	0	35
	2035.8	1	b	+	-				1	36
	1066.3	2	d	+	+					
	1077.2	2	e	+	+					
1786.7	1883.6	1	a	+	+	5	4	1	0	37
	2076.7	1	b	+	+				1	38
	1086.9	2	d	+	+				2	39
	1183.4	2	f	+	+					
	1243.4	2	e	+	+					
1827.7	1924.6	1	a	+	-	4	5	1	0	40, 41
	2117.8	1	b	+	+				1	42, 43
1868.7	1965.7	1	a	+	+	3	6	1	0	43
1882.6	1979.6	1	a	+	+	9	2	0	0	44
	1038.3	2	c	+	+					
1989.7	2086.8	1	a	+	-	5	5	1	0	45
	2279.8	1	b	+	-				1	46, 47
	1188.4	2	d	+	+				2	48
	1285.0	2	f	+	-					
2005.7	1196.4	2	d	+	+	6	5	0	1	49, 50
	1207.4	2	e	+	+				2	51, 52
	1218.3	2	g	+	+					
	1292.9	2	f	+	+					
	1303.9	2	e	+	+				3	53, 54
	1438.5	2	f	-	+					

	958.7	3	j	-	+					
2030.8	2127.7	1	a	+	-	4	6	1	0	- <sup>5</sup>
	2320.8	1	b	+	+				1	- <sup>5</sup>
2151.8	2248.8	1	a	+	+	6	5	1	0	<b>55, 56</b>
	2441.9	1	b	+	+				1	<b>57, 58</b>
	1269.4	2	d	+	+				2	<b>59, 60</b>
	1329.4	2	h	+	+				3	<b>61, 62</b>
	1366.0	2	f	+	+					
	1426.0	2	e	+	+					
	1523.0	2	i	+	+					
	1007.4	3	j	+	+					
2192.8	2289.8	1	a	+	-	5	6	1	0	- <sup>5</sup>
	2482.9	1	b	+	-				1	- <sup>5</sup>
2354.9	1371.1	2	d	+	+	6	6	1	1	- <sup>5</sup>
	1467.5	2	f	+	+				2	- <sup>5</sup>
2370.9	1379.0	2	d	+	+	7	6	0	1	<b>63</b>
	1475.5	2	f	+	+				2	<b>64</b>
	1621.0	2	f	+	+				3	<b>65</b>
2516.9	1452.0	2	d	+	+	7	6	1	1	<b>66</b>
	1512.0	2	h	+	+				2	<b>67</b>
	1548.5	2	f	+	+				3	<b>68</b>
	1608.5	2	e	+	+				4	<b>69</b>
	1064.7	3	k	+	+					
	1694.1	2	f	+	+					
	1705.1	2	i	+	+					
	1754.1	2	e	+	+					
	1765.1	2	g	+	+					
	1129.1	3	j	+	+					
	1839.6	2	f	+	+					
	1850.6	2	i	+	+					
	1226.1	3	j	+	+					
	1233.4	3	l	-	+					
2882.0	1634.6	2	d	+	+	8	7	1	1	<b>70</b>
	1731.1	2	f	-	+				2	<b>71</b>
	1876.6	2	f	-	+				3	<b>72</b>
	1250.8	3	j	-	+				4	<b>73</b>
	1347.8	3	j	1	+					
3247.2	1372.5	3	j	1	+	9	8	1	3	<b>74</b>

1) Monoisotopic mass of the neutral glycan

2)  $m/z$  of measured ion

3) Ionic composition: a)  $[M+H_2PO_4]^-$ , b)  $[M-H]^-$ , c)  $[M+(H_2PO_4)_2]^{2-}$ , d)  $[M-H+H_2PO_4]^{2-}$ , e)  $[M-H_2+Na+H_2PO_4]^{2-}$ , f)  $[M-H_2]^{2-}$ , g)  $[M-H_3+Na_2+H_2PO_4]^{2-}$ , h)  $[M-H_2+Na+(H_2PO_4)_2]^{2-}$ , i)  $[M-H_3+Na]^{2-}$ , j)  $[M-H_3]^{3-}$ , k)  $[M-H_2+H_2PO_4]^{3-}$ , l)  $[M-H_4+Na]^{3-}$

4) As in Scheme 1.

5) Insufficient fragmentation data to assign structures (probably bisected triantennary or tetra-antennary glycans lacking various galactose residues).

## Legends for Figures and Scheme

**Scheme 1.** Structures of the glycans identified in the gp120 samples. Symbols for the structures are:

■ = GlcNAc, ● = mannose, ◆ = galactose, ◆ = fucose, ★ = Neu5Ac (sialic acid). The angles of the lines joining the symbols denote the linkage positions: | = 2-link, / = 3-link, - = 4-link and \ = 6-link. Alpha bonds are shown with dashed lines and beta bonds with full lines. Further details are given in the paper by Harvey *et al.* [66]. Fragment ions are named according to the system proposed by Domon and Costello [56].

**Figure 1.** (a) DriftScope display ( $m/z$ :drift time) for *N*-glycans from gp120. Regions enclosed by ovals are singly charged ions (1), doubly charged ions (2) and triply charged ions (3). (b) Negative ion ESI spectrum of *N*-glycans released from the glycoprotein gp120. (c) Negative ion ESI spectrum of low concentrations of *N*-glycans released from the glycoprotein gp120. (d) Mobility-extracted singly charged ions from Sample 2 (from region 1 of panel a). (e) Mobility-extracted doubly charged ions from Sample 2 (from region 2 of panel a). (f) Mobility-extracted triply charged ions from Sample 2 (from region 3 of panel a). Conventions for the structural diagrams and fragment ion labelling in this and the other figures are as in the legend to Scheme 1. Ions are labelled with the most abundant peak of the isotope cluster. Where two isomers of the triantennary glycans were detected, only one is shown because of lack of space. All detected isomers are shown in Scheme 1 and Table 1.

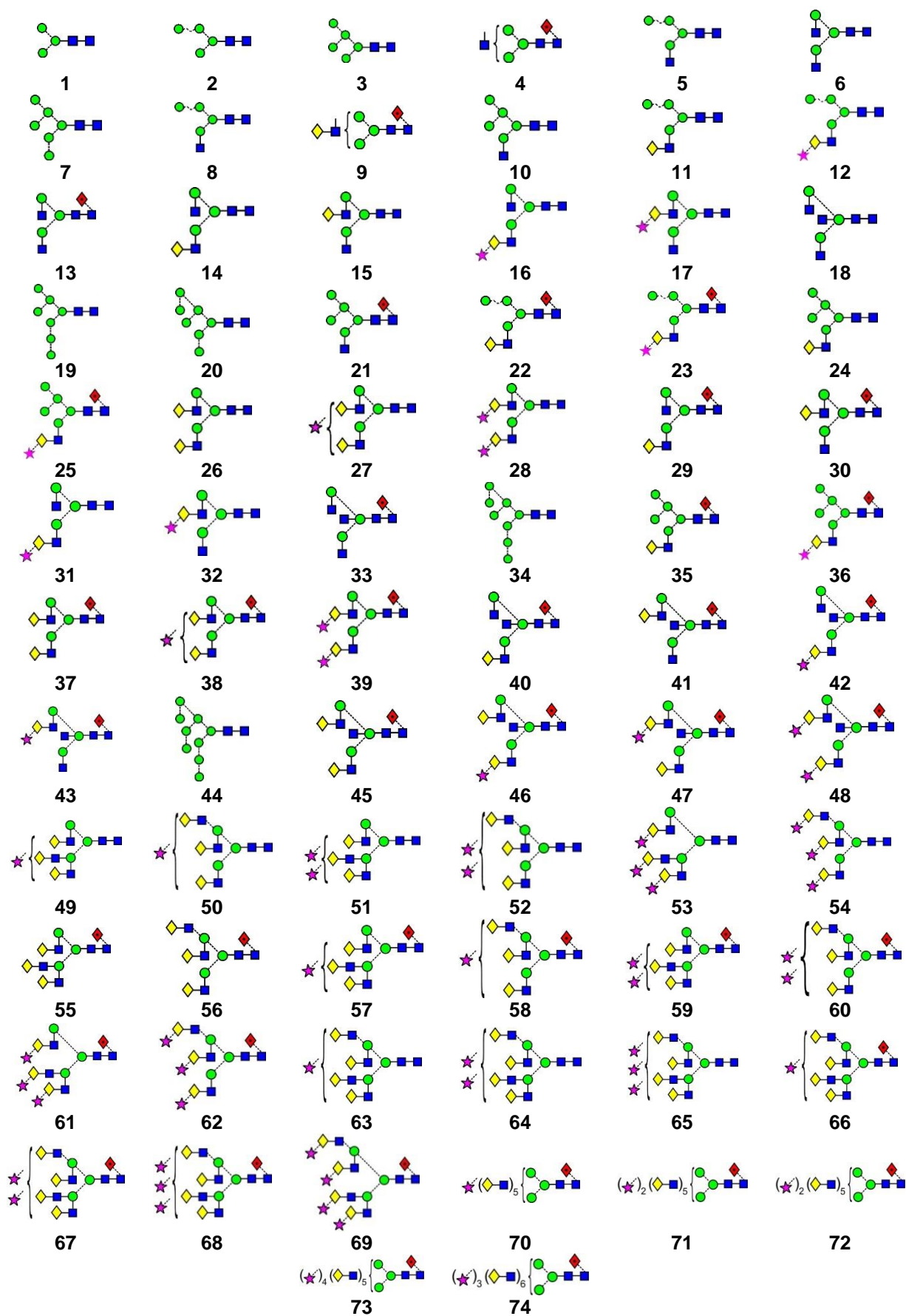
**Figure 2.** (a) Negative ion CID spectrum (transfer cell) of the ion at  $m/z$  1721 from the sample of gp120 glycans whose ESI spectrum is shown in Figure 1d. The inset shows the ATD profile (red trace) and two diagnostic ions from each of the two main constituents. The horizontal lines show the regions that were extracted to produce the spectra shown in panels b and c. (b) Mobility-extracted CID spectrum of the phosphate adduct of the biantennary glycans Gal<sub>1</sub>Man<sub>3</sub>GlcNAc<sub>4</sub>Fuc<sub>1</sub> (**29**, **30**, region b from the inset above). (c) Mobility-extracted CID spectrum of the CID spectrum of the <sup>2,4</sup>A<sub>6</sub> fragment ion ( $m/z$  1720) from the high mannose glycan Man<sub>9</sub>GlcNAc<sub>2</sub> (**3**, region c from the inset above). (d) Mobility-extracted CID spectrum of the phosphate adduct of the biantennary glycans Gal<sub>1</sub>Man<sub>3</sub>GlcNAc<sub>4</sub>Fuc<sub>1</sub> (**29**, **30**) from the spectrum shown in Figure 1b (high concentration sample). (e) Mobility-extracted CID spectrum of the CID spectrum of the <sup>2,4</sup>A<sub>6</sub> fragment ion ( $m/z$  1720) from the high mannose glycan Man<sub>9</sub>GlcNAc<sub>2</sub> (**3**) from the spectrum shown in Figure 1b.

**Figure 3.** (a) Negative ion CID spectrum (transfer fragmentation) of the ion at  $m/z$  1979 corresponding to the phosphate adduct of the high mannose glycan, Man<sub>9</sub>GlcNAc<sub>2</sub> (**44**). (b) Mobility extracted CID spectrum from the boxed region of the DriftScope plot shown below in panel c. (c) Extracted contaminating ions. The inset shows the  $m/z$ :drift time (DriftScope) display with the boxed area containing the fragment ions from Man<sub>9</sub>GlcNAc<sub>2</sub> (**3**). Section b of the inset shows the corresponding ATD plot.

**Figure 4.** (a, Inset) ATD plot (red trace) of the ion at  $m/z$  1534 from gp120 together with selected diagnostic fragment ions (blue and green traces) for the two glycans shown in panels b and c respectively. (a) CID spectrum of the ion at  $m/z$  1534. (b) Mobility extracted CID spectrum (transfer region) of the phosphate adduct of the hybrid glycan **10**. (c) Mobility extracted CID spectrum (transfer region) of the phosphate adduct of the hybrid glycan **11**.

**Figure 5.** (a) Negative ion CID spectrum of the ion at  $m/z$  1007 from gp120. (b) Mobility-extracted CID spectrum (singly charged) of the trimannosyl-chitobiose glycan **1** from region 1 of the drift time: $m/z$  (DriftScope) plot shown in Figure 6. Spectra of the regions 2-6 of the DriftScope plot are shown in panels c-g respectively. The inset to panel d shows the CID spectrum of the tri-sialylated triantennary glycans **61**, **62** recorded with a collision cell voltage of 55 V.

**Figure 6.** (a) DriftScope display ( $m/z$ :drift time) of transfer region CID fragments from  $m/z$  1007 following mobility separation. (b) Corresponding ATD plot. The peak from the Man<sub>3</sub>GlcNAc<sub>2</sub> glycan (**1**) is labelled.



Scheme 1



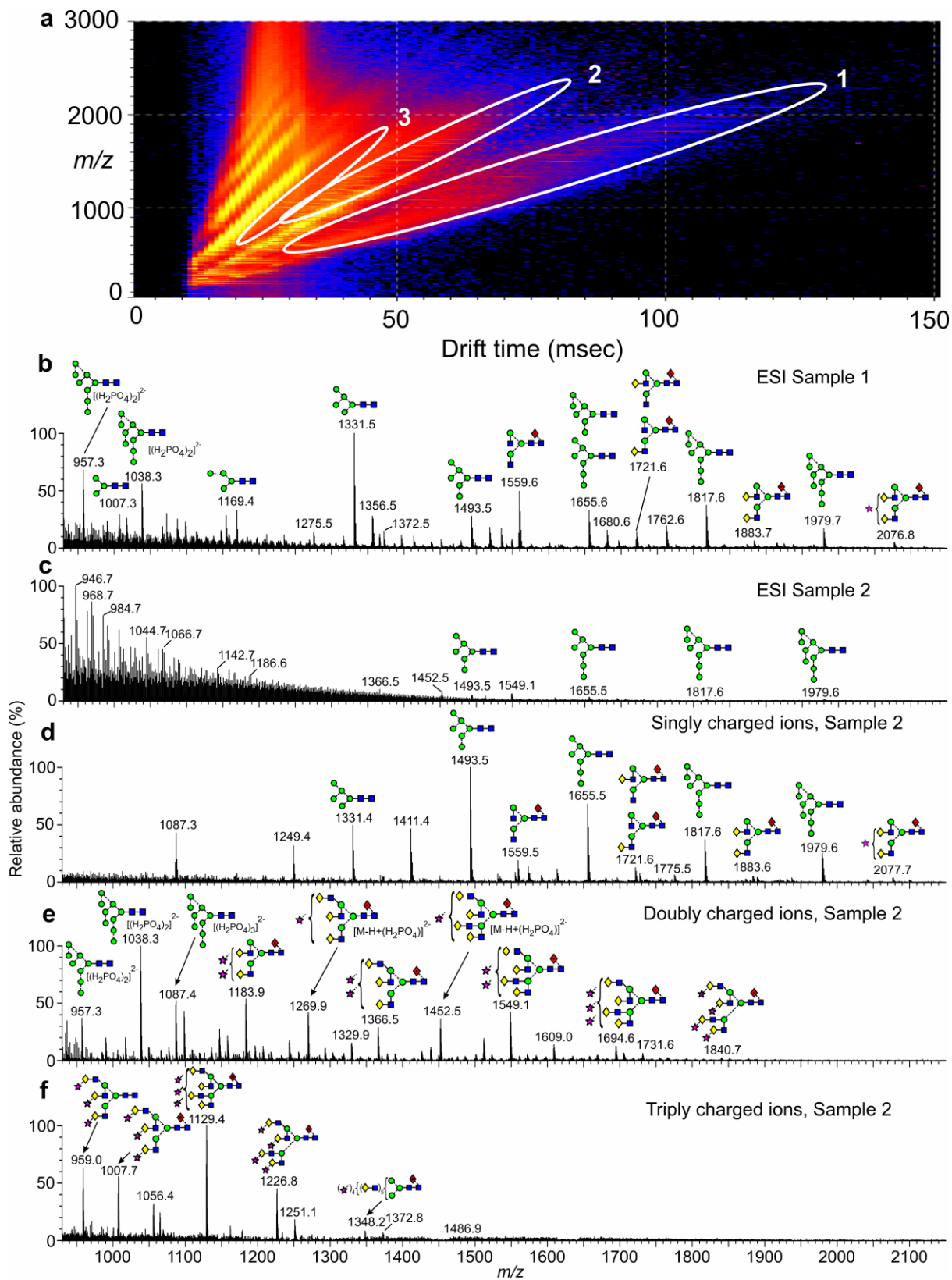


Figure 1





Figure 2

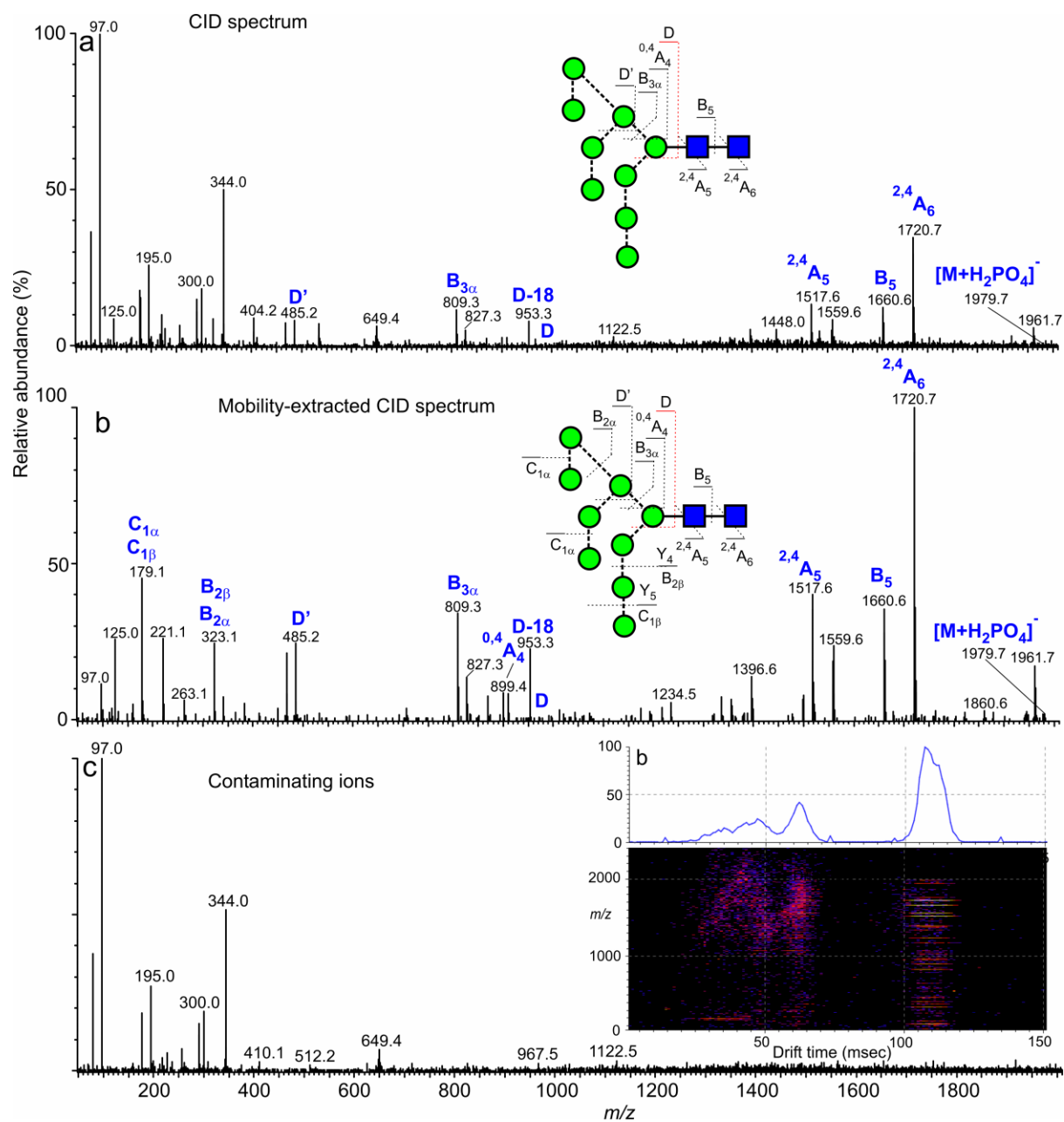


Figure 3

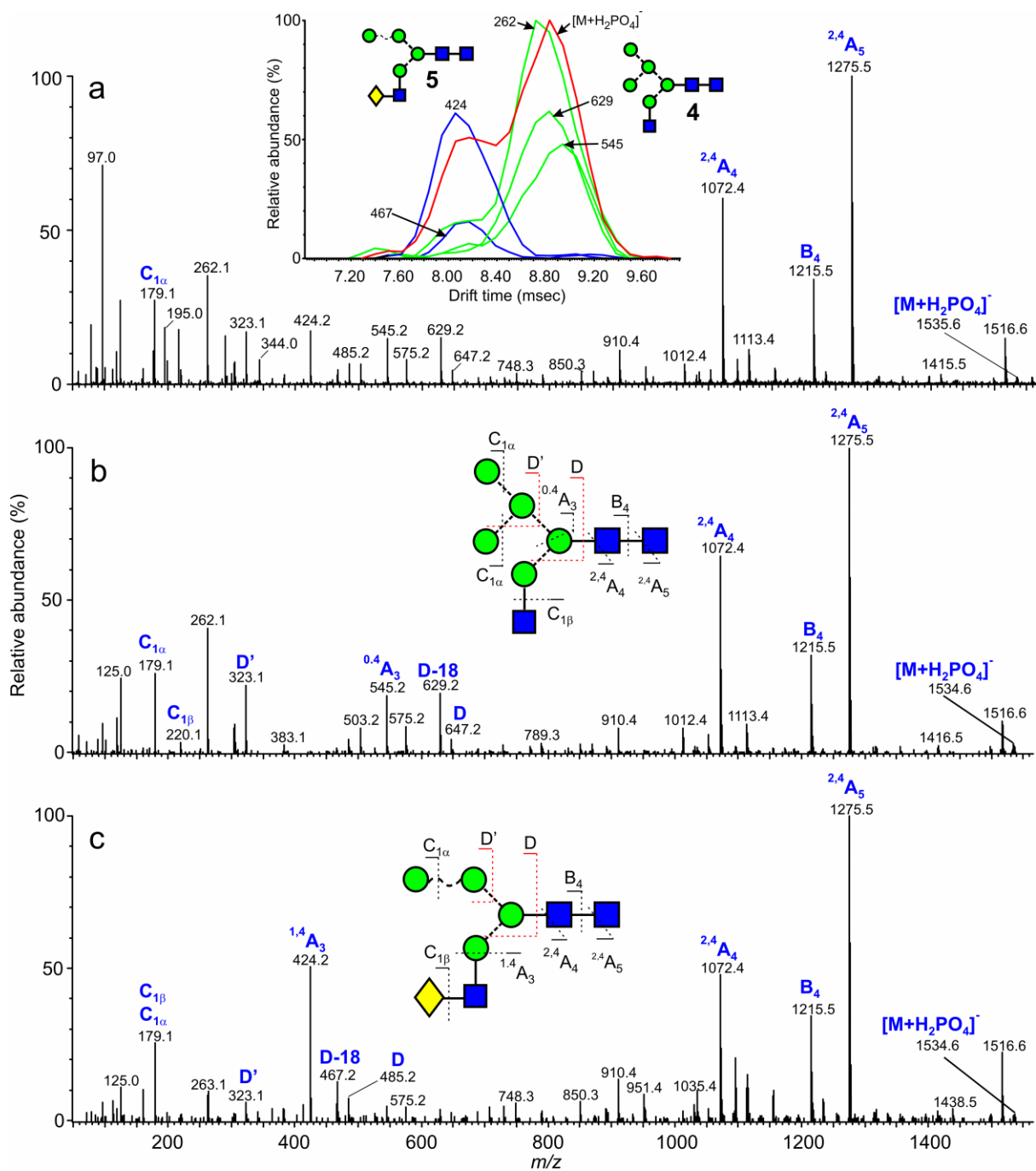


Figure 4

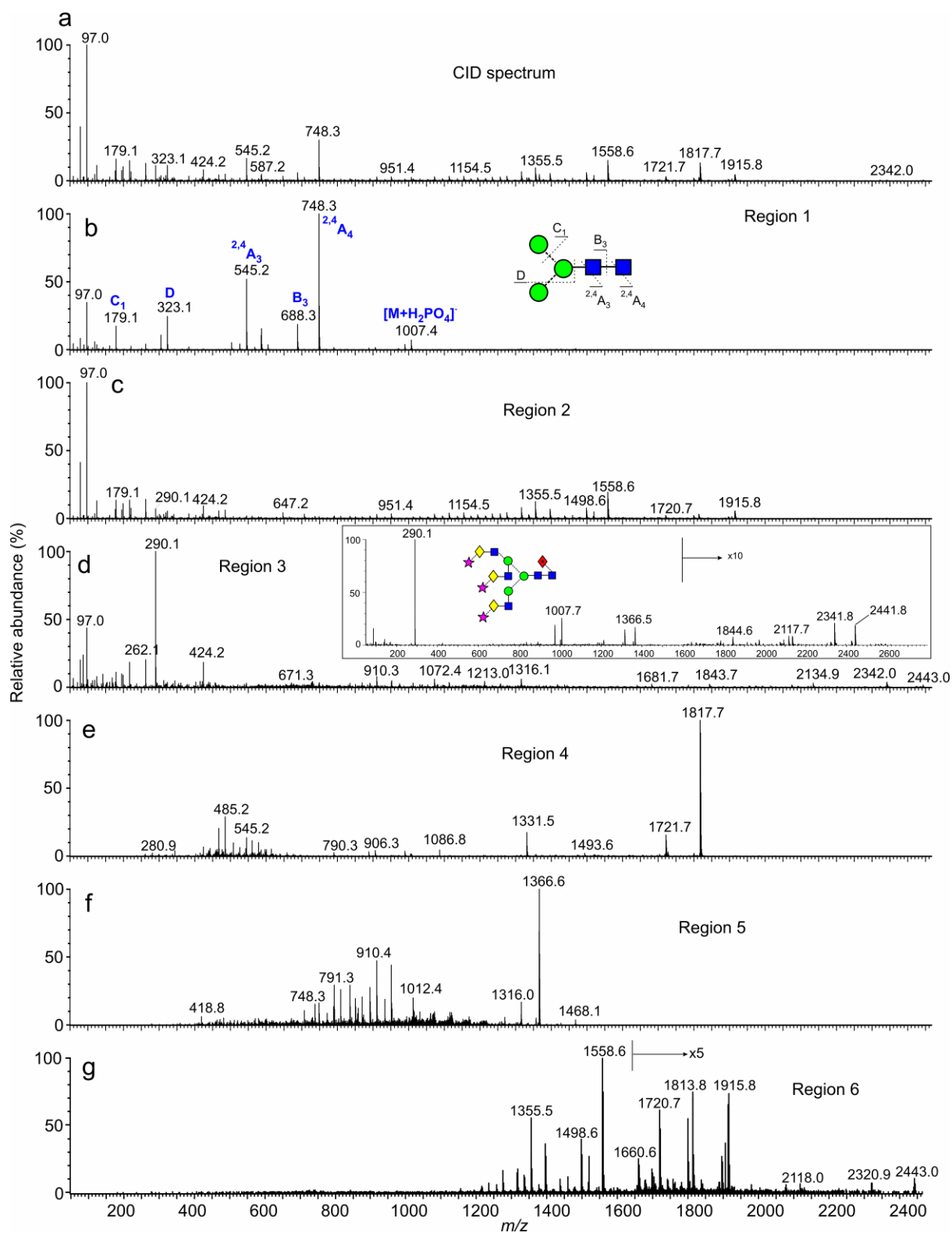
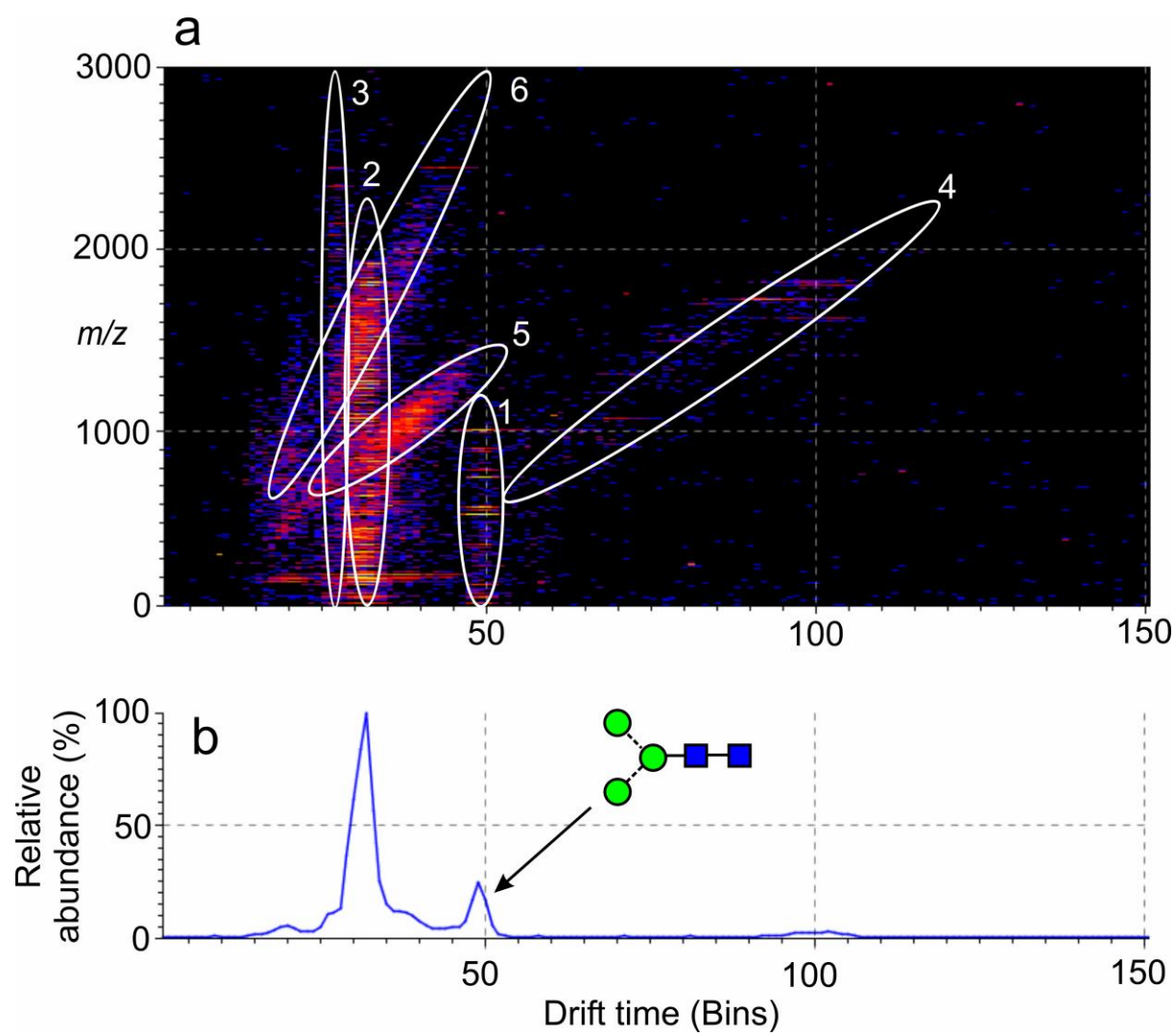
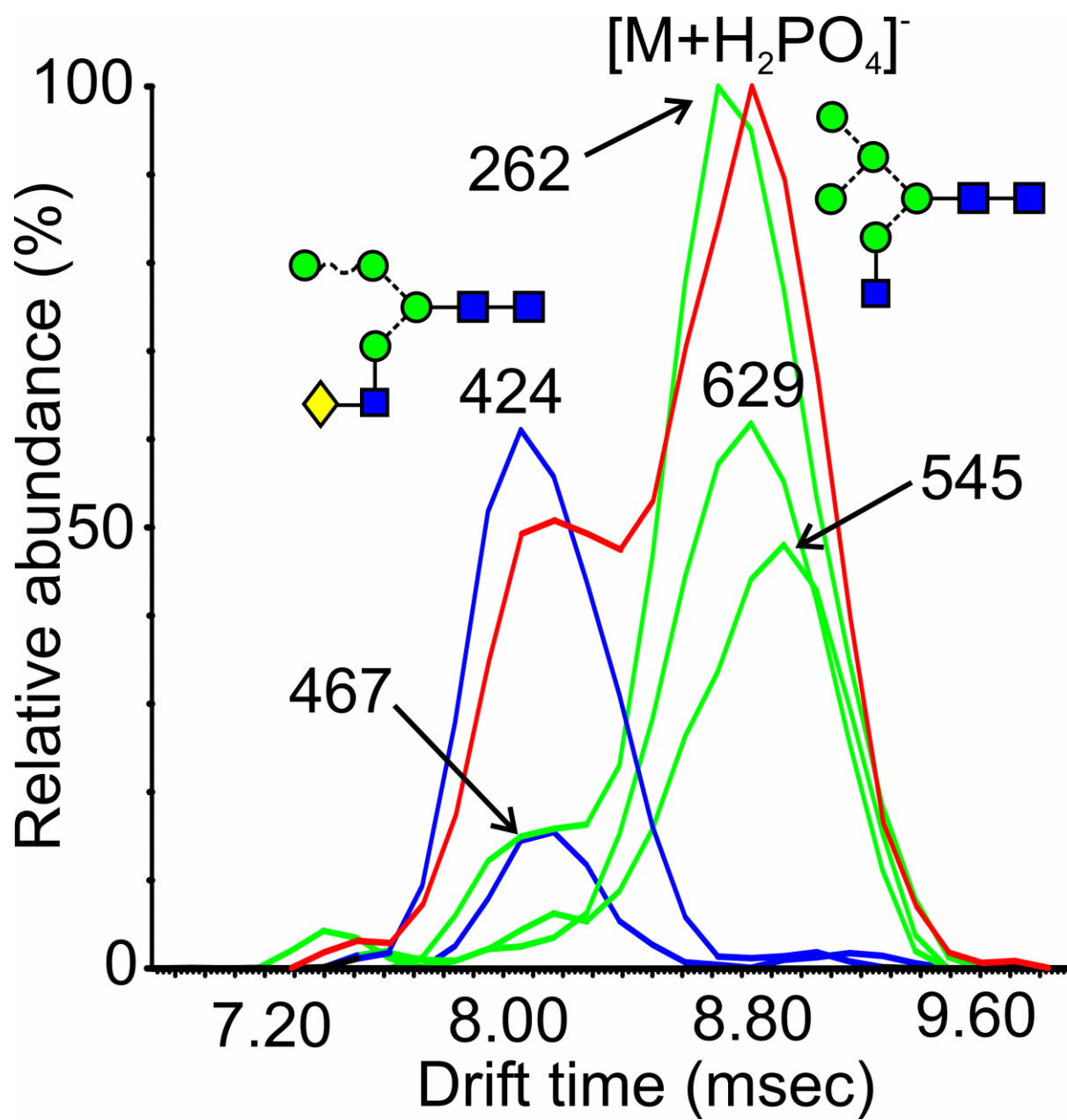


Figure 5





Graphical abstract